NASA Technical Memorandum 86729

A Comparison of Measured and Calculated Thermal Stresses in a Hybrid Metal Matrix Composite Spar Cap Element

Jerald M. Jenkins, Allan H. Taylor, and I. Frank Sakata

September 1985

National Aeronautics and
Space Administration

NASA Technical Memorandum 86729

A Comparison of Measured and Calculated Thermal Stresses in a Hybrid Metal Matrix Composite Spar Cap Element

Jerald M. Jenkins
Ames Research Center, Dryden Flight Research Facility, Edwards, California
Allan H. Taylor
Langley Research Center, Hampton, Virginia
I. Frank Sakata
Lockheed California Company, Burbank, California

1985

National Aeronautics and
Space Administration
Ames Research Center
Dryden Flight Research Facility
Edwards, California 93523

A COMPARISON OF MEASURED AND CALCULATED THERMAL STRESSES IN A HYBRID METAL MATRIX COMPOSITE SPAR CAP ELEMENT

by

Jerald M. Jenkins
NASA Ames Research Center
Dryden Flight Research Facility
Edwards, California

Allan H. Taylor
NASA Langley Research Center
Hampton, Virginia

and

I. Frank Sakata
Lockheed California Company
Burbank, California

INTRODUCTION

The potential for the use of metal matrix composite materials in structural applications is, in many respects, proportional to such factors as the extent of material characterization, the practical experience with the material, and the applicability of computational methods. The content of this paper is directed toward adding to the general knowledge of these factors with particular emphasis on the prediction of thermal stresses in a hybrid metal matrix composite spar cap element (references 1 and 2). The need to critically evaluate computational procedures has increased in recent years because the cost of laboratory testing and test specimens has resulted in a deficiency of test data providing a basic comparison of calculated and measured thermal stresses (reference 3). The wide spectrum of configuration/material options has also contributed to this deficiency.

A hybrid metal matrix composite upper surface wing spar cap element (reference 2) composed of titanium which was selectively reinforced with boron-carbide-coated boron filaments in an aluminum matrix was used as a specimen to

compare computed thermal stresses with measured values obtained from a thermal cycling experiment. The instrumented test component was heated in an oven and the thermal strains resulting from dissimilar material effects were measured. The metal matrix composite portion of the spar is an orthotropic unidirectionally reinforced fibrous composite material. A finite element NASTRAN (reference 4) model with appropriate anisotropic elements was developed to provide computational data for comparative purposes. Rules of mixtures were utilized to estimate anisotropic elastic and expansive properties and these results were incorporated into the structural model for comparison with experimental results.

SYMBOLS

E	Young's modulus, Pa (lbs/in^2)
$f(t)$, $g(T)$	non-linear mathematical representations
G	shear modulus, Pa (lbs/in^2)
K	general linear constant
Q	stiffness constant, Pa (lbs/in^2)
T, ΔT	temperature, incremental temperature, K (F°)
V	volume fraction
α	coefficient of linear expansion, m/mK (in/inF°)
ε	strain, m/m (in/in)
ν	Poisson's ratio
σ	Stress, Pa (lbs/in^2)

SUBSCRIPTS

A	refers to apparent
c	refers to corrected value
f	refers to fiber
i,j	arbitrary numbers
m	refers to matrix
s	refers to standard
M	refers to metal matrix composite

DESCRIPTION OF TEST

The origin of the hybrid titanium/metal matrix composite test specimen and the associated reasoning behind the configuration is well documented in reference 2. The specimen is configured to be associated with the upper spar cap area as is depicted in figure 1. The fibers are oriented unidirectionally along the longitudinal axis of the test specimen. The 1.09 meter (36.0 inch) specimen is shown in the photograph of figure 2. This figure also shows end attachments which were installed to accommodate tensile load tests not discussed in this paper. A dimensional sketch of a segment near the middle of the specimen which locates the principal strain gages used for comparison with the structural model is shown in figure 3. Thermocouples and strain gages are located as shown in figure 4. The presence of additional strain gages which were utilized in axial load tests not presented in this paper should be noted. Foil-type resistance strain gages and Chromel-alumel thermocouples were utilized for this test.

The data presented in this paper was obtained from a single thermal cycle of a specimen that was undergoing a 200 cycle thermal exposure test in an oven. The nature of the thermal cycle is depicted in the time-history of temperature presented in figure 5. A cycle of thermal strain resulting from the elevated temperature of the specimen is also shown in figure 5. The basic test plan for each individual cycle was to raise the temperature from ambient to a value of 478 K (400 F°), maintain the temperature at this value for thirty minutes, and then return the specimen temperature to ambient within a total cycle time of two hours. A photograph of the cycling oven is shown in figure 6.

Because of the anisotropic character of the metal matrix composite, a major problem associated with this laboratory experiment was the appropriate selection of strain gages. The temperature compensation/apparent strain relations were critical since the thermal expansion properties in the three major material axes were not known precisely (this was not a problem with the titanium part of the specimen since the Ti-6Al-4V alloy has thermal expansion properties that are well documented). Strain gages mounted on the metal matrix composite transverse to the fibers (2-direction, see figure 3) were compensated for the aluminum alloy of the matrix. The strain gages on the metal matrix composite mounted parallel to the fibers (1-direction, see figure 3) were compensated for molybdenum since this readily available strain gage had a value which most closely represented what was thought to be the thermal expansion properties in the fiber direction.

The precise acquisition of laboratory strain gage test data requires more than presumptions about the thermal expansion properties. Therefore, two strain gages were mounted on a small coupon of the metal matrix composite parallel to the fibers and two more were mounted transverse to the fibers. Precise apparent strain curves were obtained by heating the coupons very slowly in an oven and recording the resulting strain. This data was used to correct the test data obtained from the hybrid titanium/metal matrix composite specimen for apparent strain. This data was also used to establish values for the

thermal coefficient of expansion which will be discussed in detail in the following section.

COEFFICIENT OF THERMAL EXPANSION

The thermal expansion coefficients for the metal matrix composite were determined from the strain gaged coupon seen in figure 7. The precisely known thermal expansion properties of the strain gages were used as the standard. The specimen with attached strain gages was heated slowly in an oven up to the test temperature of 478 K (400 F°). One pair of strain gages (1-direction) was compensated thermally for molybdenum and the other pair (2-direction) was compensated for aluminum. Another pair of strain gages compensated for molybdenum were oriented in the 2-direction on another specimen not shown. This was done because the values in the 2-direction were quite uncertain in the mind of the author. The thermal expansion properties were deduced from deviations of the strain gages on the metal matrix composite from the strain gage manufacturers predicted apparent strain curves.

Deducing the coefficient of thermal expansion of a material from attached strain gages is relatively straightforward since an accurate standard is inherent (the compensation value of the strain gage). An apparent strain curve (reference 5) is required and provided with strain gages because the coefficient of thermal expansion is not truly linear over the usable temperature range. If a strain gage of known compensation and known apparent strain is mounted to a material of unknown thermal expansion properties, then the thermal expansion properties of that material can be deduced from the deviation from the apparent strain curve using an oven test. The basic equation defining thermal displacement may be expressed as:

$$\alpha_M \Delta T = \alpha_s \Delta T + f(T) - g(T) \tag{1}$$

where the first term on the right hand side represents the linear portion of the standard material, the second term represents the non-linear deviation from the linear presumption of the first term, and the third term represents the deviation from the first two terms because the material on which the strain gage is mounted is different from the standard. If the quantity

$$f(T) - g(T) \tag{2}$$

is determined by experiment, then a linear approximation can be made and a correction term may be identified as

$$\alpha_c \Delta T \simeq f(T) - g(T) \tag{3}$$

hence

$$\alpha_M \Delta T = (\alpha_s + \alpha_c)\Delta T \tag{4}$$

or

$$\alpha_M = \alpha_s + \alpha_c \tag{5}$$

The linear coefficient of thermal expansion in the fiber direction (1-axis) of the metal matrix composite was determined from the standard and corrective values:

$$\alpha_{M_1} = \alpha_{s_1} + \alpha_{c_1} = \underset{(.0000030)}{.0000054} + \underset{(.0000005)}{.0000009} = \underset{(.0000035)}{.0000063} \tag{6}$$

The expansion coefficient in the transverse direction (2-direction) was determined using two strain gages of largely differing coefficients of thermal expansion. Hence, there were two sets of data used to determine the values. The test results indicate slightly differing values:

$$\alpha_{M_2} = \alpha_{s_2} + \alpha_{c_2} = \underset{(.0000130)}{.0000234} - \underset{(.0000020)}{.0000036} = \underset{(.0000110)}{.0000198} \tag{7}$$

and

$$\alpha_{M_2} = \alpha_{s_2} + \alpha_{c_2} = \underset{(.0000030)}{.0000054} + \underset{(.0000075)}{.0000135} = \underset{(.0000105)}{.0000189} \tag{8}$$

A nominal value of .00001935 m/mK (.00001075 in/inF°) was used for the thermal expansion coefficient in the transverse (2-axis) direction of the metal matrix composite.

A sample of the data used in determining the coefficients of thermal expansion is shown in figure 8. The manufacturers apparent strain curve, i.e., the f(T) term in equation (1), is represented by the solid lines. The deviation from the manufacturers apparent strain curve is represented by the difference between the line and the circular symbols. This deviation constitutes the g(T) term in equation (1). It should be noted that the deviation is cumulative strain and must be divided by the temperature change to arrive at a linear approximation of the change in coefficient of thermal expansion.

STRESS-STRAIN RELATIONS

The stress-strain relations in terms of stress components as a function of material properties and strain components is:

$$\sigma_i = Q_{ij}\varepsilon_j \qquad (i,j = 1, 2, 6) \tag{9}$$

Hence, for an orthotropic, unidirectional reinforced fibrous composite material:

$$\begin{Bmatrix} \sigma_1 \\ \sigma_2 \\ \sigma_6 \end{Bmatrix} = \begin{bmatrix} Q_{11} & Q_{12} & 0 \\ Q_{21} & Q_{22} & 0 \\ 0 & 0 & Q_{66} \end{bmatrix} \begin{Bmatrix} \varepsilon_1 \\ \varepsilon_2 \\ \varepsilon_6 \end{Bmatrix} \tag{10}$$

The stiffness constants are as follows:

$$Q_{11} = \frac{E_1}{(1 - \nu_{12}\nu_{21})}$$

$$Q_{12} = Q_{21} = \frac{\nu_{12}E_2}{(1 - \nu_{12}\nu_{21})} = \frac{\nu_{21}E_1}{(1 - \nu_{21}\nu_{12})} \tag{11}$$

$$Q_{22} = \frac{E_2}{(1 - \nu_{12}\nu_{21})} \qquad Q_{66} = G_{12}$$

The reciprocity relation discussed in reference 6 requires $Q_{12} = Q_{21}$ because:

$$\frac{\nu_{21}}{E_2} = \frac{\nu_{12}}{E_1} \tag{12}$$

The basic elastic properties are needed as input for the NASTRAN model since the MAT2 (reference 4) inputs require the diagonal half of the material property matrix of equation 9:

$$\begin{bmatrix} Q_{11} & Q_{12} & Q_{16} \\ & Q_{22} & Q_{26} \\ & & Q_{66} \end{bmatrix} \tag{13}$$

The relationships of equations 10 and 11 are also needed to reduce the measured strain data acquired on the metal matrix composite portion of the structure.

LAMINA ELASTIC PROPERTIES

The accurate knowledge of elastic properties in composite materials is critical to their safe and effective use. Frequently, insufficient or incomplete information is available to develop full confidence in material characterizations

and assumptions. The hybrid metal matrix composite spar which is the subject of this paper is no exception with respect to material properties. The basic elastic properties of the hybrid metal matrix composite spar constituents were obtained from the combination of known constituent material properties and rules of mixtures theory.

Young's modulus in the direction parallel to the continuous fibers (1-direction) can be presumed from the rule of mixtures (references 6 and 7):

$$E_1 = E_f V_f + E_m V_m \tag{14}$$

The volume ratio V_f and V_m were determined to be 0.5 from photomicrographs (reference 2). Based on constituent material properties, the value of E_1 was determined to be 242.0×10^9 Pa (35.1×10^6 lbs/in^2).

The elastic modulus transverse to the fiber direction (2-direction) was computed from the formula:

$$E_2 = \frac{E_f E_m}{V_m E_f + V_f E_m} \tag{15}$$

The value of E_2 was determined to be 110.9×10^9 Pa (16.1×10^6 lbs/in^2).

The shear modulus for the metal matrix composite, G_{12}, was estimated from the equation (reference 6):

$$G_{12} = \frac{G_m\{G_f(1 + V_f) + G_m(1 - V_f)\}}{G_f(1 - V_f) + G_m(1 + V_f)} \tag{16}$$

The relationships,

$$G_f = \frac{E_f}{2(1 + \nu_f)} \qquad G_m = \frac{E_m}{2(1 + \nu_m)} \tag{17}$$

yield the individual values for the fiber and the matrix respectively. The magnitude of G_{12} was estimated to be 59.61×10^9 Pa (8.65×10^6 lbs/in^2).

The rules of mixtures for Poisson's ratio and the individual fiber and matrix properties can be used to arrive at a value for ν_{12}:

$$\nu_{12} = V_m \nu_m + V_f \nu_f \tag{18}$$

The values $V_m = V_f = 0.5$, $\nu_m = .33$, and $\nu_f = .13$ lead to the value for ν_{12} which is computed to be $\nu_{12} = .23$.

Since the compliance matrix is symmetric, then:

$$\frac{\nu_{12}}{E_1} = \frac{\nu_{21}}{E_2} \qquad \nu_{21} = \frac{\nu_{12}E_2}{E_1} = .11 \tag{19}$$

Summarizing the basic elastic properties used for analysis:

$E_1 = 241.9 \times 10^9$ Pa (35.1×10^6 lbs/in^2)

$E_2 = 110.9 \times 10^9$ Pa (16.1×10^6 lbs/in^2)

$G_{12} = 59.6 \times 10^9$ Pa (8.65×10^6 lbs/in^2)

$\nu_{12} = .23$

$\nu_{21} = .11$

The matrix of stiffness constants developed in equations 10 and 11 can be computed from the previous basic elastic properties:

$$\begin{bmatrix} 178.6 & 19.4 & 0 \\ 19.4 & 84.1 & 0 \\ 0 & 0 & 59.6 \end{bmatrix} \times 10^9 \text{ Pa}$$

or in English units:

$$\begin{bmatrix} 25.90 & 2.81 & 0 \\ 2.81 & 12.20 & 0 \\ 0 & 0 & 8.65 \end{bmatrix} \times 10^6 \text{ lbs/in}^2$$

The use of the matrix of stiffness constants is discussed in the next section where the structural model used for predictions is presented.

STRUCTURAL MODEL

A finite element model of the hybrid metal matrix composite spar element was developed using NASTRAN (reference 4). A sixty plate element (CQUAD2), sixty-eight grid point model was developed for a symmetrical half of the spar.

The schematic of the model is shown in figure 9. The model was specifically contructed to correlate with strain gages on the actual specimen. The metal matrix composite material is represented by twelve plate elements in the 1-2 plane. All elements in the 1-3 plane are titanium. The only loading input to the model was a temperature change at the grid points consisting of the difference between room temperature and the maximum oven temperature of 478K (400 F°). The stiffness constants developed in the previous section are used as input to NASTRAN MAT2 cards in the bulk data deck.

RESULTS AND DISCUSSION

The basic thrust of this paper has been directed toward evaluating analytical methods to predict thermal stresses in a reinforced fibrous composite material. Since the test structure was a relatively simple component, the structural modeling turned out to be relatively straightforward while the definition of the material properties of the metal matrix composite was deceptively complicated. The degree of correlation of predicted thermal stresses with measured values will tend to reflect how well the metal matrix composite material was characterized rather than how well the overall spar was modeled.

Thermal strain measurements were taken on the hybrid metal matrix composite spar at the time indicated in figure 5 at locations corresponding to elements A, B, and C (figures 9 and 10). The two elements in the 1-3 plane, elements A and C, represent titanium parts of the spar while the element in the 1-2 plane, element B, represents the metal matrix composite part of the spar. The circular symbols shown in figure 10 represent thermal stresses obtained by reducing strain data obtained from strain gages mounted on the spar during the thermal cycling. Values for the elastic properties used to reduce the strain gage data are presented in the test measurement row in Table I. The solid lines shown in figure 10 represent computed thermal stresses based on the structural model shown in figure 9. The anisotropic elastic properties are determined in the Lamina Elastic Properties Section and are presented in Table I.

The correlation between predicted and measured values of thermal stresses should be viewed with the recognition that the metal matrix composite and its constituents have not been acceptably characterized. This has great impact on the results since Young's modulus and Poisson's ratio are used in the reduction of the strain data and in the computations developed with the structural model. An anisotropic structure is particularly sensitive to variations in material properties. These effects have apparently led to some large errors in correlating measured and calculated thermal stresses.

Data of a different computational nature is presented also in Table I that provides insight into the role that the anisotrophy and the material property inaccuracy of the metal matrix composite play in the thermal stress computation. The basic structural model was rerun for the same temperature case, however, the material properties for the metal matrix composite were presumed to be isotropic. In one case the metal matrix composite elements were presumed to be isotropic with the elastic and expansional properties

corresponding to those in the 1-direction. The other case was run using only the 2-direction properties (refer back to the Lamina Elastic Properties Section and the Coefficient of Thermal Expansion Section). The resulting correlation is seen (Table I) to degrade significantly from the anisotropic to the isotropic analysis. Since the change that has occurred is a material property change, it must be concluded that failure to account for anisotrophy and failure to accurately characterize the material are most likely dominant factors in the correlation of measured and computed thermal stresses of the hybrid metal matrix composite spar presented in this paper. This illustrates clearly the importance and necessity of a well defined, meaningful materials characterization prior to concept or computational tool assessments.

CONCLUDING REMARKS

A hybrid spar of titanium with an integrally brazed composite consisting of an aluminum matrix reinforced with boron-carbide-coated boron fibers was heated in an oven and the resulting thermal stresses were measured. Uniform heating of the spar in an oven resulted in thermal stresses arising from the effects of dissimilar materials and the anisotrophy of the metal matrix composite. The thermal stresses were calculated from a finite element structural model using anisotropic material properties deduced from constituent properties and rules of mixtures.

Comparisons of calculated thermal stresses with measured thermal stresses on the spar are presented. It was shown that failure to account for anisotrophy in the metal matrix composite elements would result in large errors in correlating measured and calculated thermal stresses. It was also concluded that very strong material characterization efforts are required to predict thermal stresses well in anisotropic composite structures.

NASA Ames Research Center
Dryden Flight Research Facility
February 28, 1985

REFERENCES

1. Sakata, I.F.; and Davis, G.W.: Evaluation of Structural Design Concepts for an Arrow-Wing Supersonic Cruise Aircraft. NASA CR-2667, April, 1977.

2. Sakata, I.F.; Davis, G.W.; and Cox, J.M.: Advanced Hybrid Structural Concepts Development - Technology Study for Advanced Supersonic Cruise Vehicles. NASA CR-3728, 1983.

3. Wagner, R.E.; Stultz, J.W.; Lee, R.C.; and Wilkinson, R.D.: Development of Design Criteria and Procedures to Account for the Effects of Elevated Temperatures Upon Missile Airframes - Tasks I, II, and III. AFWAL-TR-82-3099, December, 1982.

4. NASA-COSMIC: NASTRAN Users Manual. NASA SP-221(05), 1978.

5. Jenkins, Jerald M.: A Study of the Effect of Apparent Strain on Thermal Stress Measurement for Two Types of Elevated Temperature Strain Gages. NASA TM-84904, February, 1983.

6. Whitney, James W.; Daniel, Isaac,; and Pipes, R. Byron: Experimental Mechanics of Fiber Reinforced Composite Materials; Society for Experimental Stress Analysis, Monograph No. 4, 1982.

7. Jones, Robert M.: Mechanics of Composite Materials. McGraw-Hill Book Company, 1975.

8. Jenkins, Jerald M.; Schuster, Lawrence S.; and Carter, Alan L.: Correlation of Predicted and Measured Thermal Stresses on a Truss-Type Aircraft Structure. NASA TM-72857, 1978.

9. Jenkins, Jerald M.: Correlation of Predicted and Measured Thermal Stresses on an Advanced Aircraft Structure with Similar Materials. NASA TM-72862, 1979.

10. Jenkins, Jerald M.: Correlation of Predicted and Measured Thermal Stresses on an Advanced Aircraft Structure with Dissimilar Materials, NASA TM-72865, 1979.

TABLE I. — SUMMARY OF MATERIAL PROPERTIES AND THERMAL STRESSES

(a) Material properties

ELASTIC PRESUMPTION	TITANIUM			METAL MATRIX COMPOSITE					
	α	E	ν	α_1	α_2	E_1	E_2	ν_{12}	ν_{21}
Isotropic (1-direction properties)	9.5×10^{-6} (5.3×10^{-6})	100.0×10^9 (14.5×10^6)	.31 (.31)	19.4×10^{-6} (10.8×10^{-6})	19.4×10^{-6} (10.8×10^{-6})	82.0×10^9 (11.9×10^6)	82.0×10^9 (11.9×10^6)	.11 (.11)	.11 (.11)
Isotropic (2-direction properties)	9.5×10^{-6} (5.3×10^{-6})	100.0×10^9 (14.5×10^6)	.31 (.31)	6.3×10^{-6} (3.5×10^{-6})	6.3×10^{-6} (3.5×10^{-6})	173.7×10^9 (25.2×10^6)	173.7×10^9 (25.2×10^6)	.23 (.23)	.23 (.23)
Anisotropic	9.5×10^{-6} (5.3×10^{-6})	100.0×10^9 (14.5×10^6)	.31 (.31)	6.3×10^{-6} (3.5×10^{-6})	19.4×10^{-6} (10.8×10^{-6})	241.9×10^9 (35.1×10^6)	110.9×10^9 (16.1×10^6)	.23 (.23)	.11 (.11)
Test Measurement	NA NA	100.0×10^9 (14.5×10^6)	.31 (.31)	NA NA	NA NA	241.9×10^9 (35.1×10^6)	110.9×10^9 (16.1×10^6)	.23 (.23)	.11 (.11)
SI Units (English Units)	m/mK (in/inF°)	Pa (lbs/in^2)	none none	m/mK (in/inF°)	m/mK (in/inF°)	Pa (lbs/in^2)	Pa (lbs/in^2)	none none	none none

(b) Thermal stress

ELASTIC PRESUMPTION	ELEMENT A	ELEMENT B		ELEMENT C
	σ_1	σ_1	σ_2	σ_1
Isotropic (1-direction properties)	49.5×10^6 (7185)	76.5×10^6 (-11100)	40.0×10^6 (-5810)	62.5×10^6 (9060)
Isotropic (2-direction properties)	-27.2×10^6 (-3940)	43.2×10^6 (6260)	24.8×10^6 (3600)	-36.4×10^6 (-5280)
Anisotropic	-28.8×10^6 (-4174)	26.8×10^6 (3880)	45.2×10^6 (-6560)	-39.5×10^6 (-5730)
Test Measurement	-24.5×10^6 (-3550)	45.2×10^6 (6550)	-70.9×10^6 (-10280)	-26.9×10^6 (-3900)
SI Units (English Units)	Pa (lbs/in^2)	Pa (lbs/in^2)	Pa (lbs/in^2)	Pa (lbs/in^2)

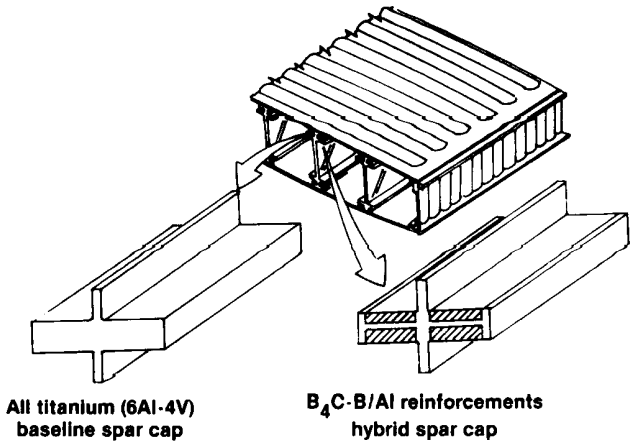

Figure 1. Alternate spar cap design concept.

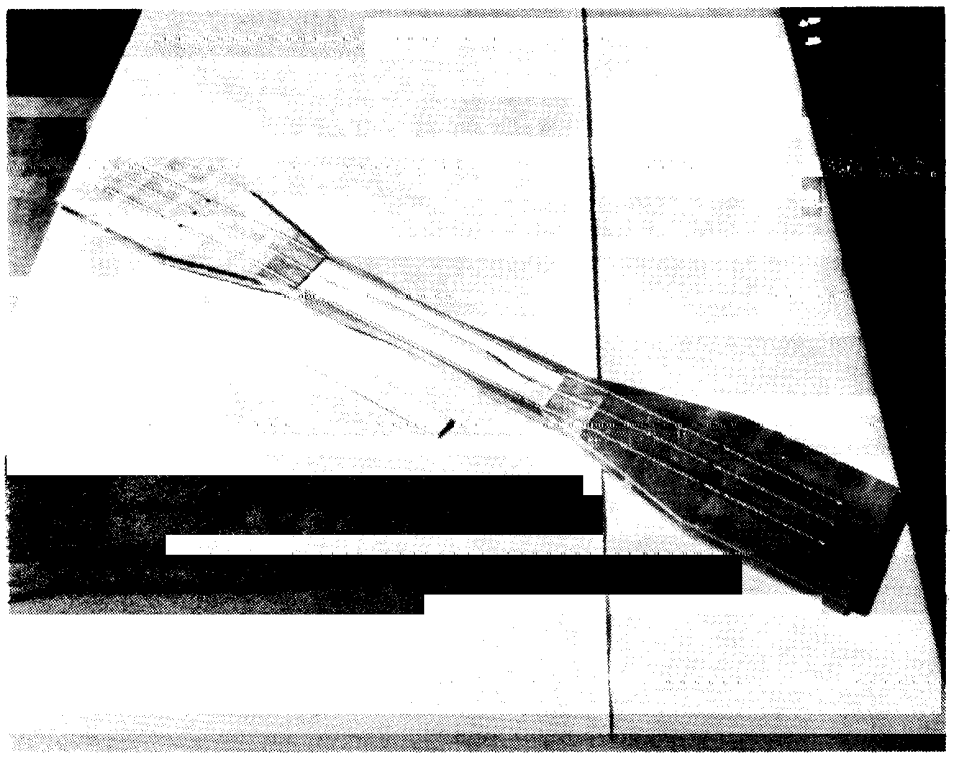

E39905

Figure 2. Test specimen for hybrid metal matrix composite spar cap.

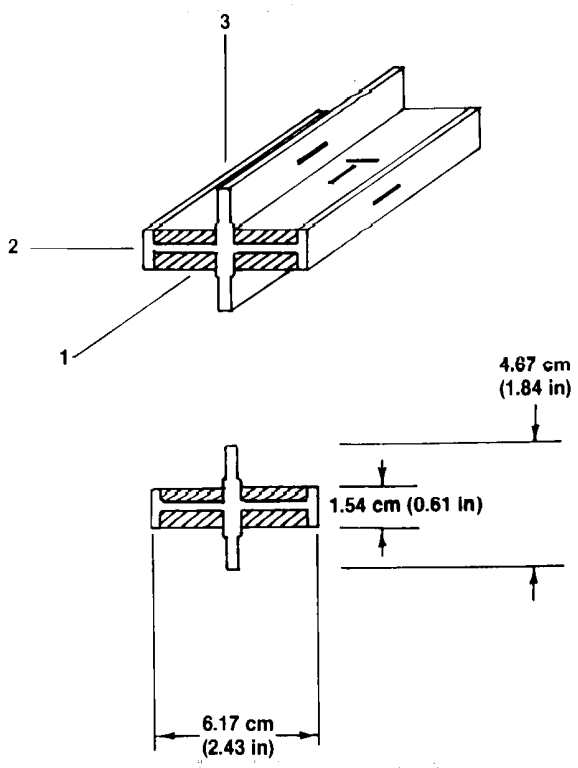

Figure 3. Detail of hybrid metal matrix composite spar cap.

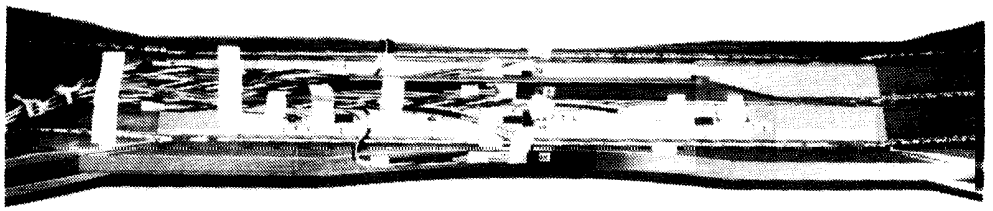

E40027

Figure 4. Instrumentation installation on spar cap test specimen.

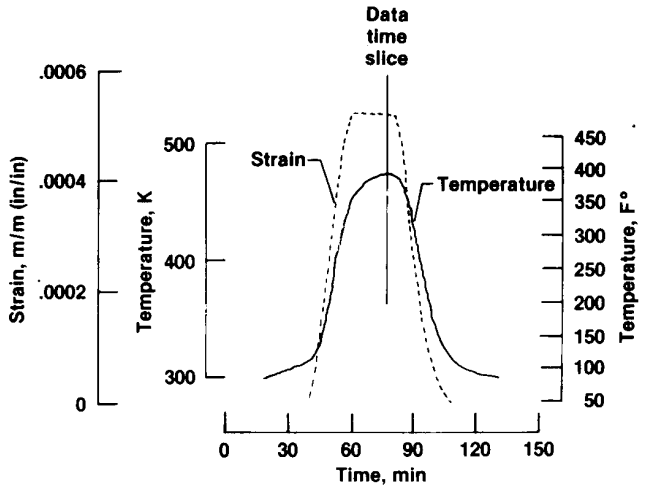

Figure 5. Time history of temperature and strain during a single thermal cycle.

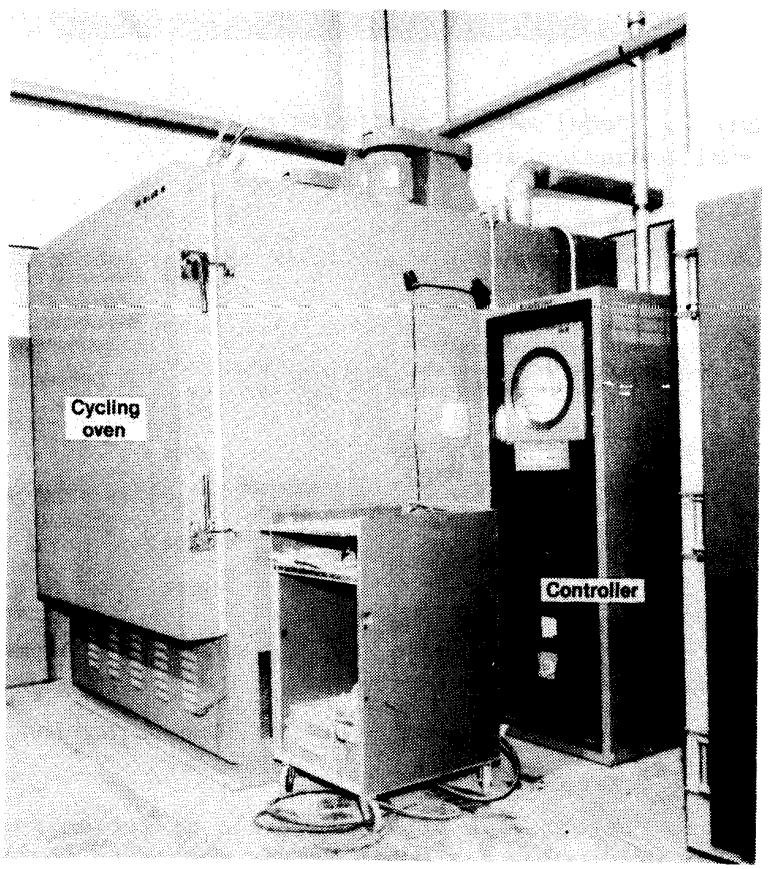

ECN28374

Figure 6. Thermal cycling oven and temperature controller.

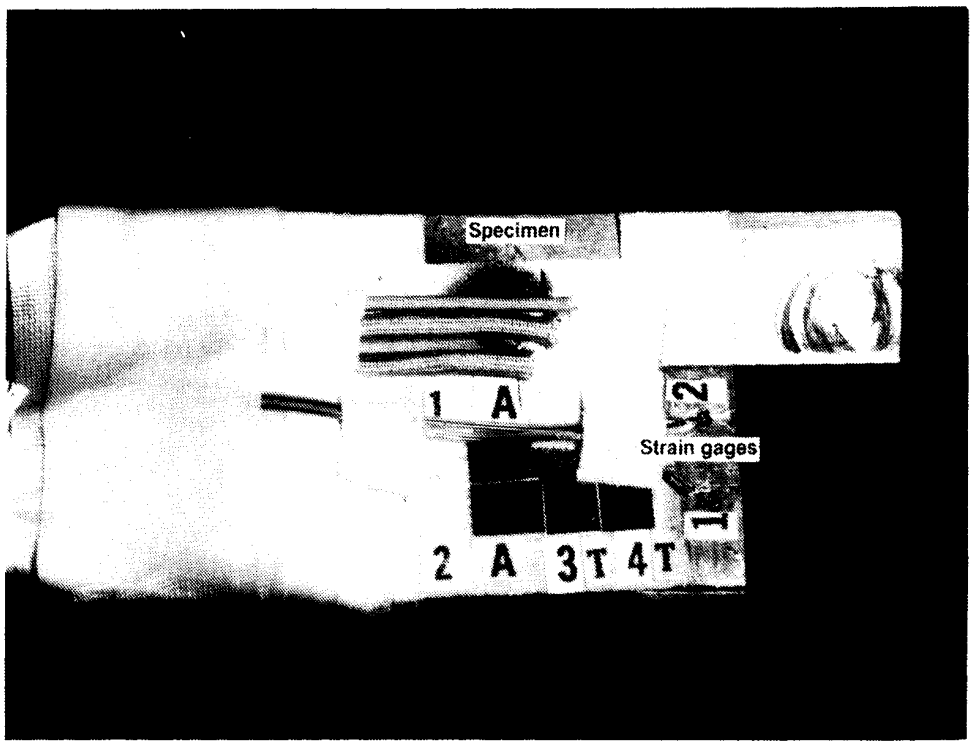

ECN26868

Figure 7. Metal matrix composite coupon used to determine thermal expansion properties.

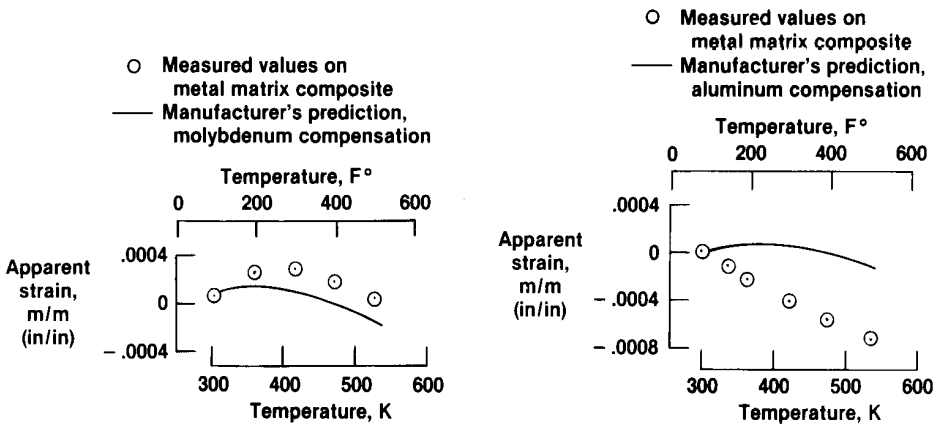

(a) Two-direction thermal expansion.

(b) One-direction thermal expansion.

Figure 8. Strain gage apparent strain deviation from manufacturer prediction for metal matrix composite coupons.

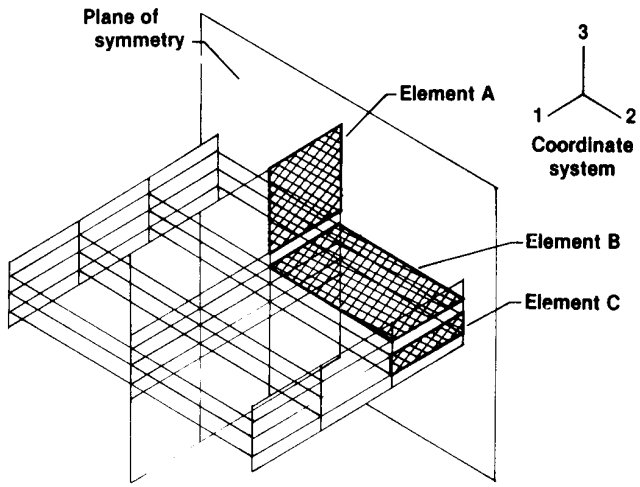

Figure 9. Finite element model of hybrid metal matrix composite spar cap.

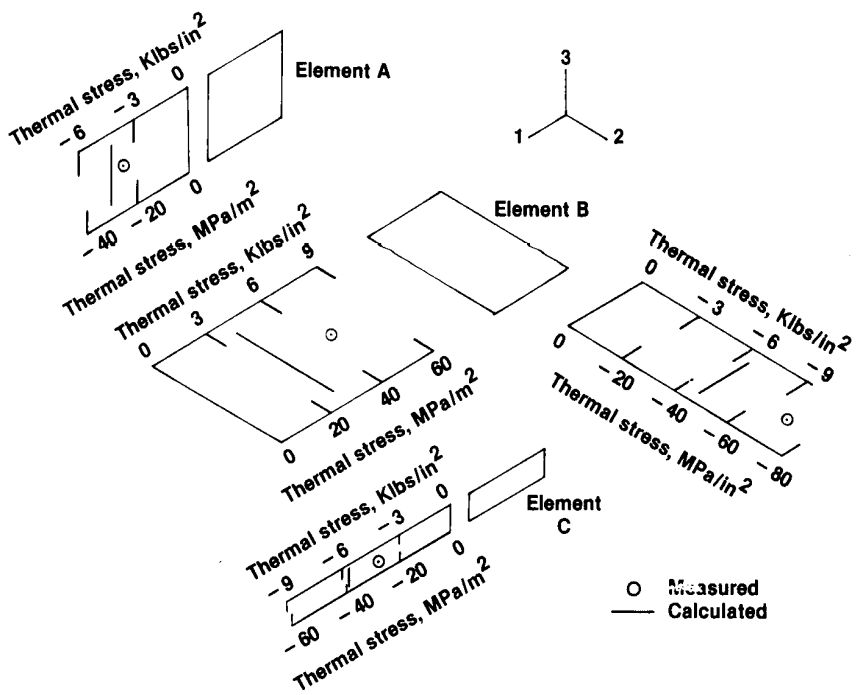

Figure 10. Comparison of measured and calculated thermal stresses.

1. Report No.	2. Government Accession No.	3. Recipient's Catalog No.
NASA TM-86729		

4. Title and Subtitle	5. Report Date
A Comparison of Measured and Calculated Thermal Stresses in a Hybrid Metal Matrix Composite Spar Cap Element	September 1985
	6. Performing Organization Code
7. Author(s) Jerald M. Jenkins, Allan H. Taylor, and I. Frank Sakata	8. Performing Organization Report No. H-1289
	10. Work Unit No. RTOP 506-53-51
9. Performing Organization Name and Address NASA Ames Research Center Dryden Flight Research Facility P.O. Box 273 Edwards, CA 93523-5000	11. Contract or Grant No.
	13. Type of Report and Period Covered Technical Memorandum
12. Sponsoring Agency Name and Address National Aeronautics and Space Administration Washington, D.C. 20546	14. Sponsoring Agency Code

15. Supplementary Notes

Jerald M. Jenkins is affiliated with NASA Ames Research Center, Dryden Flight Research Facility, D-OFS, Edwards, California 93523-5000. Mr. Taylor is affiliated with NASA Langley Research Center; Mr. Sakata is affiliated with Lockheed California Company, Burbank, California.

16. Abstract

A hybrid spar of titanium with an integrally brazed composite, consisting of an aluminum matrix reinforced with boron-carbide-coated fibers, was heated in an oven and the resulting thermal stresses were measured. Uniform heating of the spar in an oven resulted in thermal stresses arising from the effects of dissimilar materials and the anisotrophy of the metal matrix composite. Thermal stresses were calculated from a finite element structural model using anisotropic material properties deduced from constituent properties and rules of mixtures. Comparisons of calculated thermal stresses with measured thermal stresses on the spar are presented. It was shown that failure to account for anistrophy in the metal matrix composite elements would result in large errors in correlating measured and calculated thermal stresses. It was concluded that very strong material characterization efforts are required to predict accurate thermal stresses in anisotropic composite structures.

17. Key Words (Suggested by Author(s))	18. Distribution Statement
Material properties Metal matrix composite Thermal stress	Unclassified – Unlimited STAR category 39

19. Security Classif. (of this report)	20. Security Classif. (of this page)	21. No. of Pages	22. Price*
Unclassified	Unclassified	19	A02

For sale by the National Technical Information Service, Springfield, Virginia 22161.